

Statistical analysis of excitation energies in the actinide and rare-earth nuclei

A.I. Levon,^{*} A.G. Magner,[†] and S.V. Radionov[‡]

Institute for Nuclear Research, 03680 Kyiv, Ukraine

(Dated: July, 1st, 2017)

Statistical analysis of distributions of the excited state energies in the actinide and rare-earth nuclei is performed in terms of the nearest neighbor spacing distributions. Several approximations, such as the linear approach to the level-repulsion density and that suggested by Brody, to these distributions were applied for the analysis. We found an intermediate character of the experimental spectra of the excitation energies between the order and the chaos for a number of rare-earth and actinide nuclei. They are more close to the Wigner distribution for energies limited by 3 MeV, and to the Poisson distribution for data including higher excitation energies and higher spins. As follows from the cumulative distributions, the Wigner contribution dominates at smaller spacings while the Poisson one is more important at larger spacings.

I. INTRODUCTION

The microscopic many-body interaction of particles of the systems, such as heavy deformed nuclei, is rather complicated. Therefore, several theoretical approaches to the description of nuclear excitations are helpful for understanding the properties of the collective motion in such nuclei. As the simplest approaches, one can mention the calculations within the phenomenological interacting-boson model [1] and a more microscopic quasiparticle-phonon model [2]. Toward the microscopic picture, there are several other approaches based on the mean-field approximation, like the Hartree-Fock theory with, in addition, taking into account the residue interactions and applying the cranking model [3, 4]. However, one can significantly simplify the realistic many-body problem and enrich its understanding by using the nuclear models which are based on the statistical properties of the distributions of discrete levels.

Different statistics have been proposed to exhibit the statistical properties of systems in relation to the regular (Poisson statistics) and chaotic (Gaussian ensemble statistics) limits. At the same time, the nearest-neighbor spacing distribution (NNSD) statistics is mostly common used to analyze the short-range fluctuation properties in the observable spectra. An absolutely regular uniform sequence of the energy levels is described by the Poisson distribution. If there is a pure repulsion of the energy levels, they suppress spectral fluctuations, and the energy intervals between levels can be described by the Wigner distribution.

To get information on the degree of chaos in the energy spectra, a comparison of the NNSDs with the well-known Brody [5, 6] and Berry-Robnik [7] distributions is often carried out by the least-square fit technique over one parameter. However, for instance, the Brody distribution, as an interpolation between the Wigner and the Poisson distribution, is in fact heuristic. Because of the lack of a theoretical justification, it cannot properly serve a strict criterion of the chaos in a quantum system.

For a quantitative measure of the degree of chaoticity of the many-body forces, the statistical distributions of spacings between the nearest neighboring levels were derived within a more consequent theory which we shall call, for shortness, below as the Wigner-Dyson (WD) theory [6, 8–11]. Integrability (order) of the system was associated usually to the Poisson-like exponentially decreasing dependence of the spacing variable with a maximum at zero while chaoticity was connected more to the Wigner-like behavior with the zero spacing probability at zero but with a maximum at a finite value of this variable.

For a further study of the order-chaos properties of the nuclear systems, it might be worth to apply simple approximations to the WD NNSD. For instance, for analysis of the statistical properties in terms of the Poisson and Wigner distributions, one can use the linear WD (LWD) approximation to the level-repulsion density [12]. As a smooth analytical function, this approximation looks more founded within the WD theory (see Appendix). It gives a more proper information on the separate Poisson-like order and Wigner-like chaos contributions, in contrast to the qualitative heuristic Brody approach.

In the present work, the alternative approaches, such as the LWD approximation to the NNSD, based on the Wigner-Dyson theory, and the Brody method are used for the statistical description of the excitation energies in deformed actinide and rare-earth nuclei. They are discussed in relation to the degree of the chaoticity in terms of the Poisson and Wigner distribution contributions. In addition, the cumulative NNSDs show the statistical properties of these collective states as functions of the spacing variable in relation to the same limits.

This article is organized in the following way. In Section ??, we present the unfolding method for calculations of the NNSD directly from the experimental data. In Section ??, we outlook several analytical approximations to the NNSD within the Wigner-Dyson theory. The NNSD using the linear approximation to the level-repulsion density, and the Brody approach, and the cumulative distribution method are discussed in relation to the experimental data in Sec. IV. Our results are summarized in Sec. V. Some details of our derivations are given in Appendix.

* Email: levon@kinr.kiev.ua

† Email: magner@kinr.kiev.ua

‡ Email: sergey.radionov@matfys.lth.se

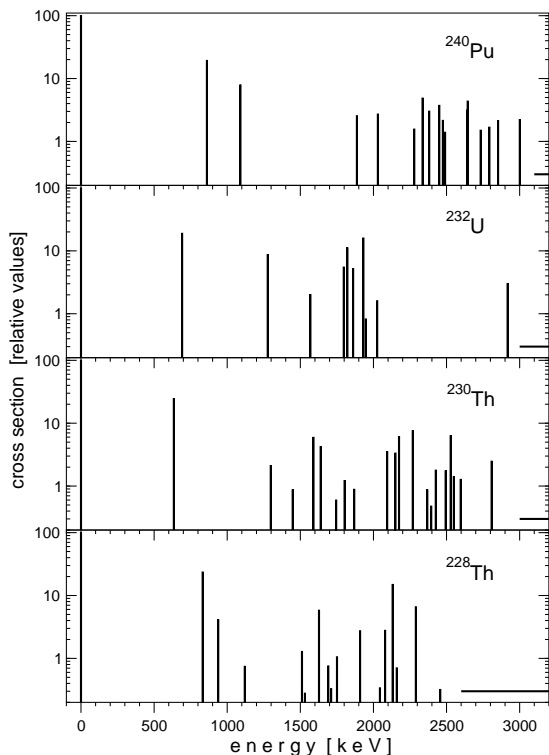


FIG. 1. The location and the (p,t) strength of 0^+ states in ^{228}Th , ^{230}Th , ^{232}U and ^{240}Pu . Horizontal lines indicate limitations in the investigation energy.

II. EXPERIMENTAL DATA AND UNFOLDING METHOD

lsec2:expunfold

To perform statistical analysis of the energy spacings, one needs the complete and pure sequences of levels, – the levels with the same angular-momentum and parity quantum numbers. For a statistical accuracy, such sequences should be long enough. They are available at the excitation of nuclei in the two-neutron transfer reactions. Most of the studies using these reactions, namely the proton-triton reactions (p,t), are devoted to the investigation of the nature of 0^+ states. In fact, the observation of the long sequences of 0^+ states is available only in such reactions. The first observation of multiple excitations with the zero angular-momentum transfer was realized for the (p,t) reaction in the odd nucleus ^{229}Pa [13]. Such studies were initiated by many collaborations, e.g., for even-even actinide [14–17] and rare-earth [18–21] nuclei. Typical spectra of 0^+ states are shown in Fig. 1. However, the use of the (p,t) reaction is not limited to the observation only of 0^+ states. The long sequences of states with the angular momenta 2^+ , 4^+ , and even 6^+ were identified for nuclei in the actinide region [14–16, 22, 23]. They can be used in the statistical analysis, too. The purity of all these sequences of states is maintained by the fact that all these states are collective by their nature. This follows, for instance, from an analysis within the framework of the interacting boson model, and the quasiparticle phonon model [14–16, 19, 24].

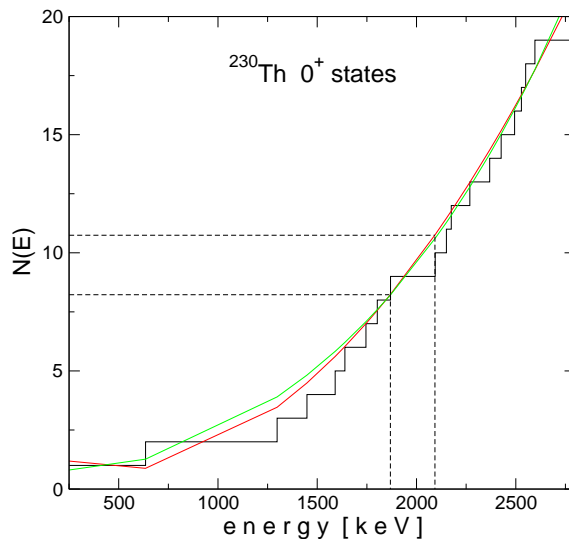


FIG. 2. Histogram of the cumulative number of states, $N(E)$, for the 0^+ energy spacings in ^{230}Th and its fitting by two smooth polynomials, $\tilde{N} = a_0 + a_1E + a_2E^2$ and $\tilde{N} = a_0 + a_1E^2 + a_2E^4$, present the method of an extraction of the normalized effective NNSD from the experimental data.

To compare properly the statistical properties of different sequences to each other, one should convert any set of the energy levels into a set of the normalized spacing, that can be done through the so-called *unfolding procedure* [25]. In this procedure, an original set of the level energies E_i , $i = 1, 2, \dots$, is transformed into a new set,

$$\varepsilon_i = \tilde{N}(E_i), \quad (1)$$

where $\tilde{N}(E)$ is a smooth part of the cumulative level density, $N(E) = \int_0^E dE' (dN/dE')$, where dN/dE is the level density. The density $N(E)$ is a staircase function which counts the number of states with energies, E , which are less or equal to a given value of E . The decomposition of the cumulative level density (or, the level density itself) into smooth and fluctuating parts is not obvious. Usually, one uses polynomial fits to a smooth part.

In what follows, the spectra will be analyzed in terms of the spacings between the unfolded energy levels (1),

$$s_i = \varepsilon_{i+1} - \varepsilon_i. \quad (2)$$

By Taylor expansion of $\tilde{N}(E_i)$ in Eq. (1) up to linear terms in $E_{i+1} - E_i$, one writes

$$\varepsilon_{i+1} - \varepsilon_i \approx (E_{i+1} - E_i) \frac{d\tilde{N}(E_i)}{dE_i} = \frac{E_{i+1} - E_i}{D_i}, \quad (3)$$

where $D_i = 1/(d\tilde{N}(E_i)/dE_i)$ is the average level spacing locally in a small vicinity of E_i . For the approximation (3), one assumes that the average spacing between the unfolded levels (1) is one, provided that the smooth level density $d\tilde{N}(E_i)/dE_i$ is a slowly varying function of the energy E_i .

Thus, for each observed level, the value of the fit function can be used to generate a spacing distribution, as illustrated in Fig. 2. As one can see, a small (large) energy spacing corresponds to a small (large) spacing in $\tilde{N}(E)$. The distribution $\tilde{N}(E)$ was then used for building the final distribution of spacings. Since the statistics data for a particular sequence is limited, we compiled the distribution for all sequences to get the entire unified set of the nearest neighbor-spacing distribution with a definite sampling interval (see Subsec. D for the specific examples).

As shown in Fig. 1, the spectrum of states is sparse and widely spread. Therefore, the polynomial fitting looks as a difficult problem. Indeed, using different polynomials to fit the full spectrum of states, one obtains a different fit at the beginning of the spectrum and, as a result, a somewhat different NNSD. The reason is in a specific property of the energy spectra: The spacing between the first levels is much larger than that between all other levels. Therefore, in the statistical analysis, the first level should be discarded. Then, the remaining smooth-state trend is well reproduced by any low-order polynomial, and various polynomials lead to a very close NNSD. In the analysis we used the following polynomials: $\tilde{N} = a_0 + a_1 E + a_2 E^2$ and $\tilde{N} = a_0 + a_1 E^2 + a_2 E^4$, where a_i are fitting parameters. Absolute values of s_i for each level, obtained with different polynomials, are distinguished somehow, but the final result for spacing distributions differ only by the part with a low statistics. Therefore, the results for both polynomials are stable and compiled well, too.

The NNSD obtained in such a way are normalized to one by using the Simpson method and, then, they are fitted by theoretical distributions.

III. WIGNER-DYSON NNSD

lsec3:WD

A. General ingredients

Following the review [6], one obtains the probability of finding the spacing s between the nearest neighboring levels, (see also Refs. [8–11], and Appendix)

$$p(s) = g(s) \exp\left(-\int_0^s g(s') ds'\right) / \aleph. \quad (4)$$

The key quantity $g(s)$ is the so called level-repulsion density, $g(s) = dN/ds$, where dN is the number of states in the interval ds from s to $s + ds$ (see Appendix). It is convenient to consider s in units of the average D of distances between levels, $s = S/D$, where S is the energy spacing, i.e., the distance between the neighbor levels in the usual energy units. Thus, D is locally a mean distance between neighboring levels in the energy units.

Practically, the normalization factor \aleph can be approximately found for a large maximal value of s , s_{\max} ,

$$\aleph = \int_0^{s_{\max}} ds g(s) \exp\left(-\int_0^s g(s') ds'\right). \quad (5)$$

This normalization factor can be relatively obtained from the normalization condition at s_{\max} going to ∞ :

$$\int_0^{s_{\max}} p(s) ds = 1. \quad (6)$$

Another normalization condition writes

$$\int_0^{s_{\max}} s p(s) ds = 1. \quad (7)$$

Notice that, for convenience, we introduced the dimensionless quantities, such as the probability distribution $p(s)$, and the level-repulsion density $g(s)$ as functions of the spacing variable s , in contrast to the notations in Ref. [6] [the probability density $P(S)$, where $S = sD$, and the level-repulsion density denoted by $r_{10}(S)$].

With the definition of the dimensionless density $g(s)$, for the uniform density one has $g(s) = 1$. This corresponds, in usual energy units, to the energy density $1/D$. The Poisson law follows if we take in Eq. (4) a constant level density

$$p_P(s) = \exp(-s). \quad (8)$$

The Wigner law follows from the assumption on a pure repulsion, i.e., on the linear level-repulsion, $g(s) \propto s$. In this case, from Eq. (4) one finds

$$p_W(s) = (\pi s/2) \exp(-\pi s^2/4). \quad (9)$$

Both distributions are normalized to one for a large maximal value of s in order to satisfy approximately Eqs. (6) and (7) and, precisely, at $s_{\max} \rightarrow \infty$.

The density $g(s)$ in fact is not a constant or simply proportional to s . The combination of the Poisson and Wigner distributions was suggested in Ref. [7] by introducing one parameter. Another level-repulsion density $g(s)$ was suggested by Brody [5].

B. A linear approximation for the repulsion density

Keeping a link with the properties of the level-repulsion density $g(s)$ (Appendix), it is convenient to define the probability $p(s)$ [Eq. (4)] for a general smooth density $g(s)$ as a polynomial of a not too large power. For the simplest statistical analysis in terms of the Poisson and Wigner-like distribution contributions, one can use the linear approximation of $g(s)$ in terms of the two free parameters a and b ,

$$g(s) = a + bs. \quad (10)$$

As applied to the level-repulsion density, this can be also supported, to some extent, by an obvious analogy with the Strutinsky smoothing procedure for calculations of the averaged level density [26, 27]. Substituting Eq. (10) into the general Wigner-Dyson formula (4) and using the normalization condition (6) with large but a finite upper limit s_{\max} (larger than the experimental data),

one obtains explicitly the analytical LWD approximation [12]:

$$p(s) = \frac{1 + bs/a}{\aleph_0 + b \aleph_1/a} \exp\left(-\frac{b}{2}s^2 - as\right), \quad (11)$$

where

$$\begin{aligned} \aleph_0 &= \int_0^c ds \exp\left(-\frac{b}{2}s^2 - as\right) \\ &= \sqrt{\frac{\pi}{2b}} \exp\left(\frac{a^2}{2b^2}\right) \left[\operatorname{erf}\left(\frac{a+bc}{\sqrt{2b}}\right) - \operatorname{erf}\left(\frac{a}{\sqrt{2b}}\right) \right], \\ \aleph_1 &= \int_0^c ds s \exp\left(-\frac{b}{2}s^2 - as\right) \\ &= \frac{1}{b} \left[1 - \exp\left(-\frac{b}{2}c^2 - ac\right) - a \aleph_0 \right], \end{aligned} \quad (12)$$

with $c = s_{\max} = S_{\max}/D$ being the maximal value of s . Then, we should satisfy the second normalization condition (7) by choosing the parameter c larger than the experimental NNSD energy (in units of D). In practice, it is convenient to perform the three-parameter fitting over parameters a , b , and c to the experimental NNSD provided that the normalization condition (7) is satisfied, and then, check that c is large enough with a good accuracy. In the limit $c \rightarrow \infty$, one has simply

$$\aleph_0 \rightarrow \sqrt{\frac{\pi}{2b}} \exp\left[\frac{a^2}{2b^2}\right], \quad \aleph_1 \rightarrow \frac{1}{b} \left[1 - a \sqrt{\frac{\pi}{2b}} \right]. \quad (13)$$

Taking the limits $a \rightarrow 1$, $b \rightarrow 0$ and $a \rightarrow 0$, $b \rightarrow \pi/2$ in Eq. (11), one simply arrives at the standard Poisson, Eq. (8), and Wigner, Eq. (9), distributions. In this way, a linear approximation (10) bridges these two limit cases through a smooth level-repulsion density. The constants a and b (after their normalization to one) measure the probability to have separately the Poisson and Wigner distribution contributions [Eq. (10)].

C. The Brody distribution

The Brody distribution can be derived analytically from Eq. (4) by assuming the following expression for the level-repulsion density:

$$g(s) = \alpha s^q. \quad (14)$$

With the normalization conditions (6) and (7), one finds [5, 6]

$$p_B(s) = \alpha(q) s^q \exp\left[-\frac{\alpha(q)}{q+1} s^{q+1}\right], \quad (15)$$

where

$$\alpha = (1+q) \left[\Gamma\left(\frac{q+2}{q+1}\right) \right]^{q+1}. \quad (16)$$

Here, $\Gamma(x)$ is the standard Gamma function, and q is a free parameter. The values $q = 0$ ($s > 0$) and $q = 1$ in Eq. (15) correspond to the same Poisson [Eq. (8)] and Wigner [Eq. (9)] distributions.

The only one parameter is an advantage of the popular distribution (15), suggested by Brody, over the approximation (11) based on the linear level-repulsion density $g(s)$. As compared to the Brody approach, the two-parametric LWD approximation (11) is, to some extent, more general and better founded within the analysis in terms of the ordered Poisson and chaotized Wigner distributions. As a linear approximation (11) for $g(s)$, it has a more clear meaning of the intermediate values of the parameters, found from the least-square fitting to the experimental NNSD. In this way, one obtains the separate Poisson and Wigner distribution contributions. This is in addition to the Brody distribution (15) based on the power density (14). Such a density [Eq. (14)] does not satisfy a smoothness property of the level-repulsion densities $g(s)$, in spite of using it in derivations of the NNSD within the WD theory (see Appendix).

Thus, the probability density (11) is a simple analytical continuation between the two Poisson and Wigner limit distributions through a smooth linear level-repulsion density $g(s)$. For a comparison and completeness, the statistical analysis of the experimentally obtained excitation-energy distributions are performed below within both the LWD and Brody approximations.

D. Cumulative NNSD

We would like to complement our NNSD analysis of nuclear spectra by the analysis using the cumulative NNSD. They are not so sensitive to a choice of a sample size Δs , as compared to the NNSD characteristics themselves. The cumulative NNSD is used as an alternative method to study the statistical properties of the experimental cumulative NNSD depending on the spacing variable s , in addition to the NNSD. In this subsection, we restrict ourselves to only a qualitative analysis by using the cumulative spacing distributions for getting the additional information about the nuclear level statistics as function of the spacing variable s . A more proper quantitative study of these statistical properties of nuclear excitations will be in a forthcoming publication.

Let us consider the cumulative nearest neighbor-spacing distribution,

$$F(s) = \int_0^s p(s') ds'. \quad (17)$$

This integral distribution is the probability to find the spacing s' between two-neighbor energy levels smaller or equal to a given value s . For the cumulative Poisson-distribution one can explicitly obtain from Eqs. (17) and (8)

$$F_P(s) = 1 - \exp(-s). \quad (18)$$

For the corresponding Wigner-distribution limit of $F(s)$, one finds

$$F_W(s) = 1 - \exp(-\pi s^2/4). \quad (19)$$

Analytical expressions for the cumulative distributions for the LWD [Eq. (11)] and the Brody [Eq. (15)] approach to the probability density will be published later.

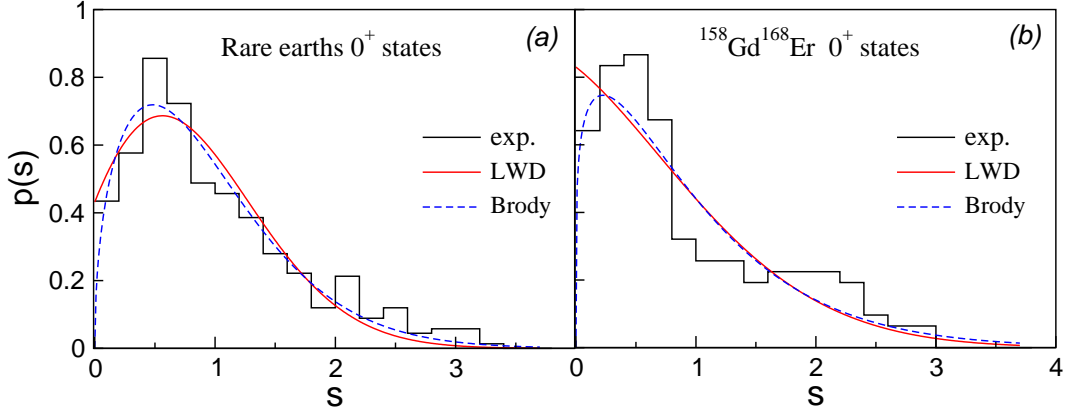


FIG. 3. Nearest neighbor spacing distributions $p(s)$ as functions of a dimensionless spacing variable, s , for 0^+ states in the rare earth nuclei and fits by the LWD approximation (red solid lines) and the Brody approach (blue dashed lines); *panel (a)* for a number of the rare earth nuclei up to the energy 3 MeV (see the text); *panel (b)* for the ^{158}Gd and ^{168}Er nuclei up to about 4 MeV. A sampling interval of $\Delta s = 0.2$ was used.

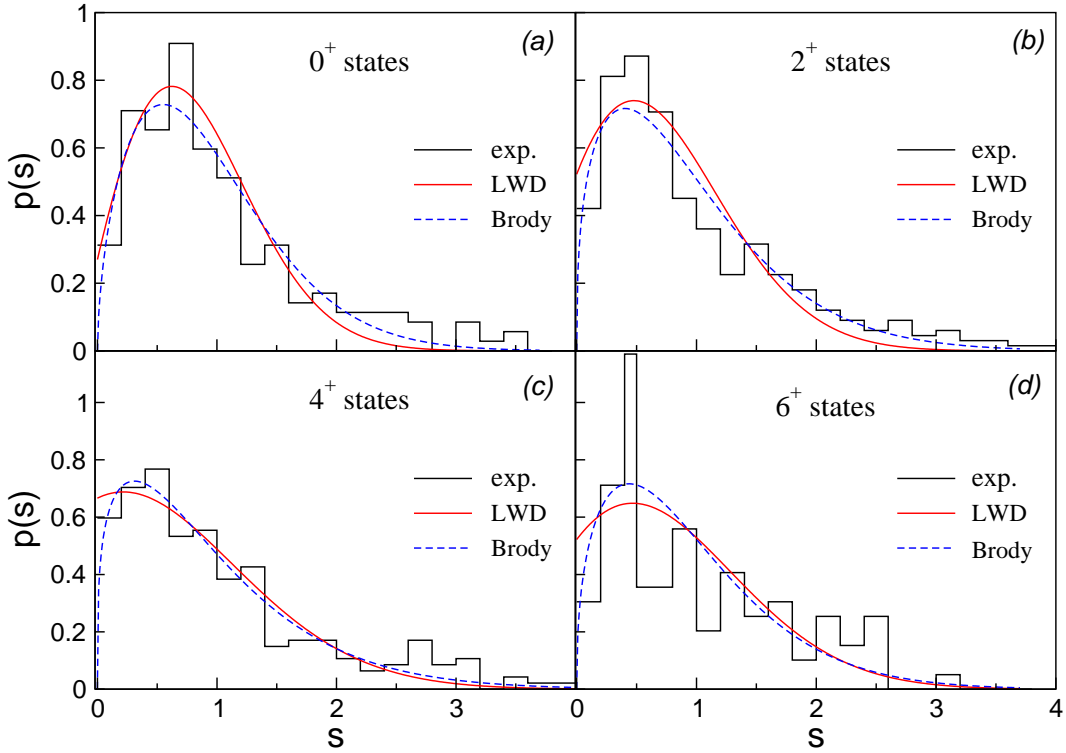


FIG. 4. The same as in Fig. 3 but for different states in the actinide nuclei; *panels (a-d)* for 0^+ , 2^+ , 4^+ , 6^+ states, respectively; and fits by the LWD (red solid lines) and the Brody (blue dashed lines) approach are shown.

IV. DISCUSSIONS OF THE FITTING RESULTS

Experimental nearest-neighbor spacing distributions fitted by the LWD approximation [Eq. (11)] and the Brody approach [Eq. (15)] are presented in Figs. 3 and

4. Parameters of fittings are given in the Table I. The sampling interval $\Delta s = 0.2$, used for building the experimental NNSD, is taken from the condition of the stable smoothed NNSD values without sharp jumps between the neighbor data. This is similar to the so-called plateau condition in the smoothing procedure for calcu-

lations of the averaged level density [26, 27]. The plateau condition means the independence of results from the averaging parameters. It also follows from the Table that the normalization condition (7) is satisfied in our calculations with good accuracy at $c \gtrsim 10$.

To build the NNSD for the rare-earth nuclei the experimental 0^+ state energies limited by the 3 MeV excitation are used for ^{158}Gd [18], ^{168}Er [19], $^{152,154}\text{Gd}$, ^{162}Dy , ^{168}Er , ^{176}Hf , $^{180,184}\text{W}$, and ^{190}Os [20], ^{170}Yb [21] nuclei [panel (a)]. The experimental NNSD for nuclei ^{158}Gd [19] and ^{168}Er [22] [panel (b)] is a special case since only for these two nuclei the measurements were carried out for larger excitation energies up to 4.2 MeV. The results of fitting are following. The rare-earth nuclear spectrum is described by 39% of the Poisson- and 61% of the Wigner-distribution contribution. They correspond approximately to the parameter $q=0.48$ in the Brody approach. At the same time, for the ^{158}Gd and ^{168}Er couple, these parameters are given by 76% and 24%, respectively, in the LWD approximation. This can be tentatively related to the value $q=0.20$ for the Brody distribution. This means that the experimental 0^+ spectra in the energy interval 0–3 MeV are intermediate between an order and a little more pronounced chaos structure, while the ordered nature is dominant for the experimental spectra in the energy interval about 0–4 MeV.

The experimental NNSDs for actinide nuclei are available also for 2^+ , 4^+ and 6^+ states, along with the 0^+ excitation states. Long sequences of 2^+ , 4^+ and even 6^+ states, as well as 0^+ states, all identified in ^{228}Th [15], ^{230}Th [14], ^{232}U [16] and ^{242}Pu [17, 23], are used in our analysis. As seen from the Table I, the picture is similar to the rare-earth behavior: All spectra in the same energy interval 0–3 MeV demonstrate an intermediate structure between an order and a chaos structure with varying dominance of the Wigner or Poisson contribution. If for 0^+ states the Wigner contribution dominates with 79 %, for the states with higher angular momenta, namely for the 2^+ and 4^+ states, the Wigner contribution is somehow lowering, and for the 4^+ states the Poisson contribution becomes dominating with 62 % ($q = 0.28$).

It looks that the results for 6^+ states violate this behavior. The Poisson contribution for them is less than for 4^+ states (although more than for 2^+ states). However, it can be explained by the features of the experimental data with increasing angular momenta to so high values. The cross section of the (p,t) reaction decreases sharply with increasing angular momenta of the final states. Therefore, a number of peaks corresponding to 6^+ states could not be distinguished. In addition, the array of the states with higher angular momenta is shifted to higher energies. With the upper limitation of the energy interval studied, this also leads to a decrease in the number of 6^+ states identified. This is particularly true for the states which correspond to small values of s : Weak peaks in a very complex and dense spectrum of tritons can be hidden in the tails of stronger nearby peaks. Further measurements for higher energies and

with a better statistics would be helpful to clarify the situation.

An increase of the Poisson distribution contribution with increasing the nuclear spin can be considered, to some extent, as that with a growth of the energy: The array of the states with higher angular momenta is shifted to larger energy excitations, too, as compared to the 0^+ case. Such a behavior would look strange when accepting that increasing the excitation energy means an increase of the temperature, or of the entropy. The entropy production could be interpreted as growing a chaos. This would mean that the Wigner distribution contribution should be greater for higher energies. However, as it was mentioned above, one can conclude about the collective nature of states excited in the (p,t) reaction, see Refs. [14, 24]. Collective excitations should not be associated with an increase of temperature. Hence, a more proper explanation of this problem should be suggested. Our results look qualitatively in agreement with the adiabatic picture of the intrinsic, vibrational, and rotational excitations in heavy deformed nuclei. In any case, the statistical analysis performed in this article provides another view on developments of a more microscopic model for the theoretical calculations.

In Fig. 5, the cumulative distributions $F(s)$ [Eq. (17)] for the 0^+ (a), 2^+ (b), 4^+ (c), and 6^+ (d) states excited in the actinide nuclei are plotted. In each panel of the Figure, the dotted line represents the corresponding cumulative Poisson distribution [see Eq. (18)]. All dashed lines in Fig. 5 show the Wigner distribution limit of $F(s)$, see Eq. (19).

As seen from this Figure, for all 0^+ , 2^+ , 4^+ and 6^+ states the Wigner cumulative distribution (19) well reproduces the behavior of empirical distributions $F(s)$ [Eq. (17)] at small and intermediate spacings s . On the other hand, at large spacings, $F(s)$ approaches basically the Poisson cumulative-NNSD limit (18). Such a peculiarity of a cumulative distribution implies a chaotic arrangements of close-lying levels and regular ones of the significantly separated levels.

As in the case of using the NNSD (see Fig. 4), the cumulative distribution analysis of Fig. 5 shows that the relative Poisson contribution (18) grows with the increase of the spin of nuclear states. It is interesting that the same tendency of the distributions $F(s)$ [Eq. (17)] with increasing spins was observed for all considered nuclei.

V. CONCLUSIONS

We provide the statistical analysis of the collective excitations with several spins: 0^+ in a number of rare-earth nuclei; and 2^+ , 4^+ , and 6^+ in a few strongly deformed actinide nuclei by using the simple approximations to the Wigner-Dyson probability distribution. These approximations to the nearest neighbor spacing distribution are based on different properties of the level-repulsion density. For the linear approximation to this density, one obtains a clear information on the quantitative measure of the Poisson order and Wigner chaos contribu-

Nuclei	States	a (%)	b (%)	$\int sp(s)ds$	Accuracy	q	Accuracy
Rare earths ^{158}Gd ^{168}Er	0^+	0.43 (39)	0.69 (61)	1.04	8.1	0.48	6.7
	0^+	0.83 (76)	0.26 (24)	0.96	11.3	0.20	10.0
Actinides	0^+	0.27 (21)	1.01 (79)	1.02	9.2	0.58	8.9
	2^+	0.52 (41)	0.75 (59)	0.95	10.2	0.38	8.2
	4^+	0.67 (62)	0.41 (38)	1.00	8.5	0.28	7.3
	6^+	0.52 (50)	0.52 (50)	1.06	14.9	0.42	13.7

TABLE I. Parameters a and b of the LWD and q of the Brody approximation for the excited states in several nuclei; the Poisson and Wigner contributions are given also as a and b normalized to 100% in circle brackets; the normalization integral of Eq. (7) at these a , b and $c \gtrsim 10$ is given too; the accuracy (χ^2) of the mean-square fitting (in percents) are shown in the 6th and 8th columns for the LWD and Brody calculations, respectively.

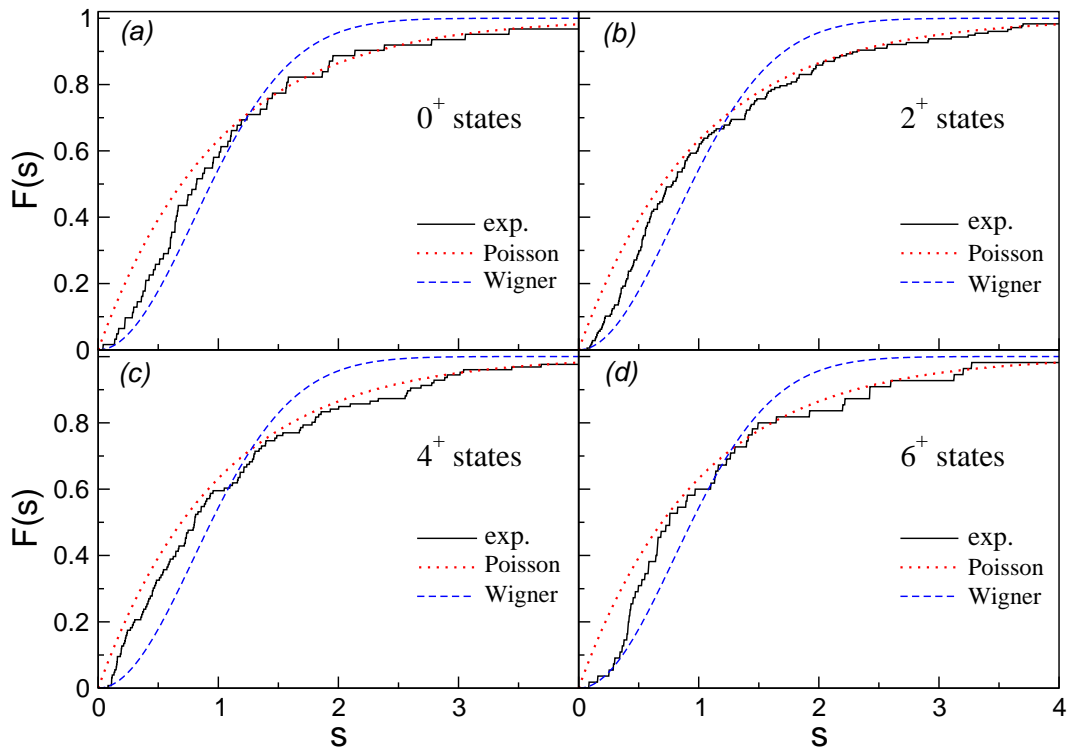


FIG. 5. Histograms of the cumulative nearest-neighbor spacing distributions (17) for the 0^+ (a), 2^+ (b), 4^+ (c) and 6^+ (d) states in the actinide nuclei discussed in Fig. 4. Dotted and dashed lines are the Poisson distribution [Eq. (18)] and the Wigner distribution [Eq. (19)] limit of these cumulative distributions (17), respectively.

tions in the experimental data, separately; in contrast to the heuristic phenomenological Brody approach. However, one finds in our calculations that the Brody formula [Eq. (15)] agrees qualitatively well with the LWD probability-distribution results [Eq. (11)].

We found the intermediate structure between the Poisson and Wigner statistical peculiarities of the experimental spectra by evaluating their separate contributions. The low energy NNSD can be described better by the Wigner distribution. The NNSD for the excitations including the higher energy region becomes more close to the Poisson distribution. Also, one finds that the Wigner contribution dominates in the NNSD for 0^+ states and

the Poisson contribution is increasing with increasing the angular momentum. This looks in line of the adiabatic picture for different excitation modes in deformed nuclei.

With the help of the cumulative distributions, we show that for the 0^+ , 2^+ , 4^+ and 6^+ states in actinide nuclei the chaotic cumulative Wigner limit well reproduces the behavior of empirical cumulative distributions $F(s)$ at small and intermediate spacings s . At larger spacings they approach the regular Poisson cumulative-distribution limit. In line of the nearest neighbor spacing distributions, the cumulative distribution analysis shows that the relative Poisson contribution grows with the increase of the spin of nuclear states.

As perspectives, we are also going to study more the Wigner-Dyson probability-density approach within simple approximations and apply them more systematically to learn the statistical properties of experimental observable data. In this way, it will be worth to calculate the cumulative nearest-neighbor spacing distributions for different approximations to the Wigner-Dyson probability distributions with getting the additional alternative information on the statistical properties of the nuclear collective states, depending on the spacing variable, angular momenta and excitation energies.

VI. ACKNOWLEDGEMENTS

We are gratefully acknowledge K. Arita, S. Aberg, J. Blocki, V.M. Kolomietz, S. Mizutori, and K. Matsuyanagi for many helpful discussions. One of us (A.G.M.) is also very grateful for kind hospitality during his working visits of Physical Department of the Nagoya Institute of Technology, also the Japanese Society of Promotion of Sciences for financial support, Grant No. S-14130.

Appendix: The derivation of the NNSD

We introduce first the level repulsion density, $g(S)$, as the number of the levels dN in the energy interval $[E + S, E + S + dS]$ divided by the energy interval length dS , $g(S) = dN/dS$ [6]. With the help of this quantity one can derive the NNSD $P(S)$ as the probability density which is a function of the spacing S between the nearest neighboring levels in energy units. Specifying $P(S)$ to the problem with the known spectra of the many-body (or single-particle, s.p.) Hamiltonian, one can split relatively a small energy interval ΔE under the investigation into many small (equivalent for simplicity) parts $\Delta S \ll \Delta E$. Each of ΔS nevertheless contain many energy levels, $\Delta S \gg D$, where D is locally the averaged distance between neighbor levels ($\Delta s \gg 1$, $s = S/D$ in the main text). Then, we find the number of the levels which occur inside of the small interval ΔS . Normalizing these numbers by the total number of the levels inside the total energy interval ΔE one obtains the distribution which we shall call as the probability density $P(S)$.

Notice that the result of this calculation depends on the energy length of the selected ΔS . In our calculations, we select ΔS by the condition of a sufficient smoothness of the distribution $P(S)$. We have to study $P(S)$ as a function of ΔS at a given S for several values of the parameters of this distribution to find a so called ‘‘plateau’’, i.e., a region of ΔS values where $P(S)$ can be approximately considered as a constant independent of ΔS and

above mentioned parameters (see Refs. [26, 27]). Such a procedure is often used for the statistical treatment of the experimentally obtained spectrum with the fixed quantum numbers as the angular momentum, parity and so on [6], see also Sec. ??.

Following mainly Ref. [11], let us calculate first the intermediate quantity $f(S)$ as the probability that there is no an energy level in the energy interval $[E, E + S]$. According to the general definition of the level repulsion density mentioned above, $g(S)dS$, can be considered as the probability that there is one energy level in the interval $[E + S, E + S + dS]$. Then, one has

$$f(S + dS) = f(S) (1 - g(S)dS) . \quad (\text{A1})$$

Assuming that $f(S)$ is a smooth function of S , one can expand $f(S + dS)$ with respect to dS . Thus, the relationship (A1) leads to the differential equation for $f(S)$,

$$df = -g(S)dSf(S). \quad (\text{A2})$$

Solving this equation, one gets

$$f(S) = C \exp \left(- \int_0^S g(x) dx \right) , \quad (\text{A3})$$

where C is arbitrary unknown constant. Note that the assumption that $f(S)$ is a smooth function of S can be satisfied if $g(S)$ is also a smooth function of S , i.e., the density $g(S)$ can be approximated by a polynomial in powers of S of not too a high power. Notice also that a constant density $g(S) = A$, and linear, $g(S) = BS$ functions of S , in which A and B are constants, obey this smoothness condition. They are related to the limit cases of the linear density $g(S) = A + BS$, namely, the Poisson (zero order polynomial, $B = 0$) and the Wigner (first order polynomial with $A = 0$) distribution functions. Let $P(S)dS$ denote the probability that the next energy level is in $[E + S, E + S + dS]$,

$$P(S)dS = f(S)g(S)dS . \quad (\text{A4})$$

Then, substituting Eq. (A3) into Eq. (A4), one finally arrives at the general distribution:

$$P(S) = Cg(S) \exp \left(- \int_0^S g(S') dS' \right) . \quad (\text{A5})$$

The boundary conditions in solving the differential equation (A2) accounts for the meaning of the NNSD $P(S)$ and its argument as the spacing between the nearest neighbor levels as shown in the integration limit in Eq. (A5). The constant C is determined by the normalization condition (6) [see Eq. (5)].

-
- [1] F. Iachello and A. Arima, *The Interacting Boson Model* (Cambridge University Press, Cambridge, England, 1987).
 [2] V. G. Soloviev, *Theory of Atomic Nuclei: Quasiparticles and Phonons* (Institute of Physics, Bristol, 1992).

- [3] P. Ring and P. Schuck, *The Nuclear Many-Body Problem* (Springer-Verlag, New York, Heisenberg, Berlin, 1980).
 [4] A. Bohr and B. R. Mottleson, *Nuclear Structure: Nuclear Deformations*, Vol. 2 (World Scientific, Singapore, 1998).

- [5] T. A. Brody, *Lett. Nuovo Cimento* **7**, 482 (1973).
- [6] T. A. Brody et al., *Rev. Mod.*, **53**, 385 (1981).
- [7] M. V. Berry and M. Robnik, *J. Phys. A* **17**, 2413 (1984).
- [8] C. E. Porter, *Statistical Theories of Spectra: Fluctuations* (Academy Press, New York, 1965).
- [9] E. P. Wigner, *Proc. Philos. Soc.*, **47**, 790 (1951).
- [10] M. L. Mehta, *Random Matrices* (Academic Press, San Diego, New York, Boston, London, Sydney, Tokyo, Toronto, 1991).
- [11] S. Aberg, *Quantum Chaos* (Mathematical Physics, Lund, 2002).
- [12] J. P. Blocki and A. G. Magner, *Phys. Rev. C* **85**, 064311 (2012).
- [13] A. I. Levon, J. de Boer, G. Graw, R. Hertenberger, D. Hofer, J. Kvasil, A. Lösch, E. Müller-Zanotti, M. Würkner, H. Baltzer, V. Grafen, and C. Günther, *Nucl. Phys. A* **576**, 267 (1994).
- [14] A. I. Levon, G. Graw, Y. Eisermann, R. Hertenberger, J. Jolie, N. Yu. Shirikova, A. E. Stuchbery, A. V. Sushkov, P. G. Thirolf, H.-F. Wirth, N. V. Zamfir, *Phys. Rev. C* **79**, 014318 (2009).
- [15] A. I. Levon, G. Graw, R. Hertenberger, S. Pascu, P. G. Thirolf, H.-F. Wirth, P. Alexa, *Phys. Rev. C* **88**, 014310 (2013).
- [16] A. I. Levon, P. Alexa, G. Graw, R. Hertenberger, S. Pascu, P. G. Thirolf, and H.-F. Wirth, *Phys. Rev. C* **92**, 064319 (2015).
- [17] M. Spieker, D. Bucurescu, J. Endres, T. Faestermann, R. Hertenberger, S. Pascu, S. Skalacki, S. Weber, H.-F. Wirth, N.V. Zamfir, and A. Zilges, *Phys. Rev. C* **88**, 041303(R) (2013).
- [18] S. R. Leshner, A. Aprahamian, L. Trache, A. Oros-Peusquens, S. Deyliz, A. Gollwitzer, R. Hertenberger, B. D. Valnion, and G. Graw *Phys. Rev. C* **66**, 051305R (2002).
- [19] D. Bucurescu, G. Graw, R. Hertenberger, H.-F. Wirth, N. Lo Iudice, A. V. Sushkov, N. Yu. Shirikova, Y. Sun, T. Faestermann, R. Krucken, M. Mahgoub, J. Jolie, P. von Brentano, N. Braun, S. Heinze, O. Moller, D. Mucher, C. Scholl, R. F. Casten, and D. A. Meyer, *Phys. Rev. C* **73**, 064309 (2006).
- [20] D. A. Meyer, V. Wood, R. F. Casten, C. R. Fitzpatrick, G. Graw, D. Bucurescu, J. Jolie, P. von Brentano, R. Hertenberger, H.-F. Wirth, N. Braun, T. Faestermann, S. Heinze, J. L. Jerke, R. Krucken, M. Mahgoub, O. Moller, D. Mucher, and C. Scholl, *Phys. Rev. C* **74**, 044309 (2006).
- [21] L. Bettermann, S. Heinze, J. Jolie, D. Mucher, O. Moller, C. Scholl, R. F. Casten, D. Meyer, G. Graw, R. Hertenberger, H.-F. Wirth, and D. Bucurescu, *Phys. Rev. C* **80**, 044333 (2009).
- [22] A. I. Levon et al., to be published.
- [23] M. Spieker et al., private communications (2017).
- [24] N. Lo Iudice, A. V. Sushkov, and N. Yu. Shirikova, *Phys. Rev. C* **72**, 034303 (2005).
- [25] O. Bohigas and M.-J. Giannoni, *Lecture Notes in Physics* **209**, 1 (1984).
- [26] V. M. Strutinsky, *Nucl. Phys. A* **95**, 420 (1967); **122**, 1 (1968).
- [27] M. Brack et al., *Rev. Mod. Phys.*, **44**, 320 (1972).